Original Article

DOI: 10.5582/bst.2022.01358

Epigenetic modification of *Kiss1* gene expression in the AVPV is essential for female reproductive aging

Ruoxi Dai[1,§], Wen Xu[1,§], Wei Chen[2], Liyuan Cui[1], Lisha Li[1], Jing Zhou[1], Xueling Jin[1], Yan Wang[1], Ling Wang[1,3,4,*], Yan Sun[1,3,4,*]

[1] Hospital of Obstetrics and Gynecology, Fudan University, Shanghai, China;
[2] Department of Urology, Zhongshan Hospital of Fudan University, Shanghai, China;
[3] The Academy of Integrative Medicine of Fudan University, Shanghai, China;
[4] Shanghai Key Laboratory of Female Reproductive Endocrine-related Disease, Shanghai, China.

SUMMARY Female reproductive senescence is heralded by hypothalamus region-specific changes in the transcription of genes such as *Kiss1* under estradiol (E2) positive feedback, associated with luteinizing hormone (LH) surge dysfunction and reproductive decline. The current study explored whether the anteroventral periventricular nucleus (AVPV) displayed epigenetic changes mediated by age-related dysregulation of gene expression and whether an epigenetic-based intervention could alleviate an aging-related neuroendocrine disorder. Chromatin immunoprecipitation sequencing (ChIP-seq) and ChIP-qPCR were used to assess the differential acetylation of histone H3 in the AVPV and the expression of genes in hormone-primed middle-aged rats. The association between acetylated histone H3 and *Kiss1* expression and the underlying mechanisms of dysregulation were determined using pharmacological inhibitors and molecular experiments *in vitro* and *in vivo*. An AVPV gene expression program failed to initiate in middle-aged females displaying typical genome-wide hypoacetylation of histone H3, and this coincided with decreased LH. Hypoacetylation of histone H3 at the 3' intergenic region of *Kiss1* in particular was associated with enhanced chromatin looping between the promoter and enhancer. Restoration of physiological histone H3 acetylation by intracerebroventricular injection of trichostatin A (TSA) restored the expression of *Kiss1* by modifying chromatin looping and led to the restoration of *Kiss1* neuronal activation and *Kiss1* synthesis as well as circulating LH. These findings have revealed novel epigenetic-associated changes in gene expression in female reproductive aging. These results also suggest that HDAC enzyme-based treatment is a potential therapeutic approach for insufficient preovulatory LH release in aging females.

Keywords aging, AVPV, estradiol, histone, acetylation, *Kiss1*

1. Introduction

Altered gene expression induced by estradiol (E2)-positive feedback in hypothalamic anteroventral periventricular nucleus (AVPV) neurons results in diminished neurotransmitter output and is well established as a key contributor to neuroendocrine changes in reproductive aging. Female reproductive aging is characterized by reduced gonadotropin-releasing hormone (GnRH) neuronal activation and dysfunction of the luteinizing hormone (LH) surge (*1-4*). Several studies have yielded findings regarding understanding of the molecular mechanisms that contribute to age-related dysregulation of genes in the AVPV. However, an unbiased view of diverse species undergoing reproductive aging has revealed that such gene alterations under E2-positive feedback were not caused by disparities among ovarian steroid exposure (*5*), altered estrogen receptor expression related to age (*6,7*), or in combination with decreased sex steroid receptors in the hypothalamus (*8*).

Epigenetic regulation, and especially histone modification, has recently been highlighted as a key mechanism to control gene expression (*9-11*) and is closely related to neuronal activation (*12*) and/or dysfunction (*13-16*). A global view of histone acetylation patterns has revealed a correlation between the level of histone acetylation at specific loci and the transcriptional activity of the gene (*17-19*). Hyperacetylation of histone in the gene promoter/enhancer region leads to chromatin organization and transcriptional activation (*20,21*).

Hypoacetylation of histone H3 in the coding region severely inhibits transcription by active genes (*20*) and may represent a critical aspect of the aging process (*22*). Moreover, histone acetylation is hypothesized to regulate binding between ERα and the estrogen response element (ERE) within the regulatory region of E2-responsive genes, mediating their transcription (*23-26*). Consistent with this hypothesis, the current authors recently reported that under E2-positive feedback conditions, acetylated histone H3 (AcH3)-immunoreactive (IR) cells in the preoptic area (POA) and AVPV increased, activating GnRH neurons for a robust LH surge (*27,28*). Of particular interest, the current authors found that females in middle age experienced differential histone H3 acetylation (H3ac) characteristics in the two nuclei as well as significant changes in HDACs (*29*), coincident with the down-regulation of *Kiss1* (anterior hypothalamus-AVPV) and a decreased LH surge (*28*). Based on these findings, more detailed and extensive information on genome-wide changes in gene expression related to acetylated histone H3 binding in the AVPV of middle-aged individuals needs to be assembled.

The *Kiss1* gene-encoded neuropeptide kisspeptin in the AVPV potently drives GnRH neuronal activation and the subsequent LH surge (*30-33*). Female rats that exhibit reproductive aging display reduced total *Kiss1* mRNA (*34*) and less *Kiss1* mRNA per cell in the AVPV as well as decreased Kiss1 cellular activation under E2-positive feedback conditions (*2*). Under E2 positive feedback, ERα recruitment and histone acetylated in the *Kiss1* promoter region consequently promote chromatin looping between the promoter and enhancer (*35,36*), which is associated with specific upregulation of AVPV *Kiss1*. However, there are few studies on the association between epigenetic changes and *Kiss1* expression in reproductive senescence. Therefore, the current hypothesis is that reduced *Kiss1* in the AVPV of middle-aged individuals may be mainly attributed to suppressed H3ac-induced chromatin loop formation, limiting the potential for interaction between a remote enhancer and a *Kiss1* gene promoter.

The current study used chromatin immunoprecipitation sequencing (ChIP-seq) analysis to characterize the contribution of altered H3ac to impaired gene expression in the AVPV of middle-aged females. The *Kiss1* and *Period 1* (*Per1*) with reduced mRNA in the AVPV were found to be epigenetically regulated *via* H3ac. Chromatin looping between the promoter and intergenic region was analyzed to determine the interaction of a *Kiss1* enhancer-promoter using chromosome conformation capture (3C) (*37,38*). Presented here is *in vivo* and *in vitro* evidence that treatment with a pharmacological histone-acetylating agent increases *Kiss1* mRNA expression and avoids age-related neuroendocrine alterations. These data provide mechanistic insight into H3ac-dependent gene expression changes in the AVPV; *Kiss1* in particular may underlie female reproductive aging characteristics, thus representing a potential therapeutic target for an LH release disorder of hypothalamic origin.

2. Materials and Methods

2.1. Animal care

Young (2-3 months) and middle-aged (9-10 months, retired breeders) female rats (Sprague Dawley, Charles River, Beijing) that were given free access to food and water were divided into groups. A 12:12 L/D cycle (lights on at 7 A.M.) was maintained. Estrous cyclicity was monitored with a daily vaginal smear for at least 2 cycles. Only rats with 2 regular estrous cycles (4-5 days) were randomly assigned to groups (*2,39,40*). All experimental procedures performed on animals were approved by the Institutional Animal Care and Use Committee of Fudan University.

2.2. Surgery and tissue harvest

2.2.1. Ovariectomy and hormone administration

After animals were anesthetized with pentobarbital sodium (30 mg/kg, ip), an ovariectomy (OVX) was performed. At 9 A.M. on day 7 after OVX, the females received a daily subcutaneous injection of 2 μg estradiol benzoate (E2; Hangxiang Inc., China) dissolved in 0.1 mL of peanut oil for two days. Forty-eight hours after the first E2 injection, the rats were treated with 500 μg of progesterone (P; Steraloids, Inc.). This hormone treatment protocol reliably stimulates neuron activation and an LH surge (*2,28,39,40*).

2.2.2. Stereotaxic surgery and cannula placement

After OVX, rats were immobilized in a RWD stereotaxic apparatus for cannula placement. A 22-gauge intracerebroventricular (icv) guide cannula (RWD Life Science, China) was positioned into the third ventricle stereotaxically (anterior/posterior + 0.2 mm; medial/lateral + 0.0 mm; dorsal/ventral - 9.8 mm relative to the bregma). A 26-gauge dummy was plugged and extended 1 mm below the guide and anchored with dental acrylic (*2,39,40*). The position of the guide cannula was confirmed by dye injection and brain sectioning to track the cannula path at the end of all experiments. Females with an accurately placed cannula were used in data analysis. A seven-day recovery was provided before animals were primed with exogenous hormone.

2.2.3. Hypothalamic dissection

The brain was quickly removed and set in a chilled stainless steel brain matrix (RWD Surgical Instrument Co.) to cut a coronal section containing the entire anterior hypothalamus, and the thickness was approximately 2

mm. The AVPV block was micro-dissected out with a microblade (Flying Eagle Razor, Gillette) and pooled in light of experimental requirements. For example, tissue from 10 young females was pooled into a single sample prior to ChIP-seq or qPCR. All tissues were frozen instantly in liquid nitrogen and transferred to a -80°C freezer.

2.3. ChIP and qPCR

2.3.1. ChIP

The ChIP-IT High Sensitivity Kit (Active motif) was used for ChIP assays. Generally, the dissected AVPV tissues were fixed with 1% formaldehyde at room temperature for 10 min, transferred into 500 μL of lysis buffer, and sonicated for 10 min. Chromatin was sheared using an Ultrasonic Processor (Sonics VCX130) and cleared by centrifugation. The solubilized chromatin was pulled down using anti-acetylated H3 (Millipore, 06-599). The beads were rinsed and the immunoprecipitated (IP) complex was eluted after incubation overnight. Libraries were constructed with IP DNA and an un-immunoprecipitated control (Input) that had been refined.

2.3.2. ChIP-seq library construction and sequencing

A NEB Ultra DNA library kit was used for library preparation, for which 50 ng of each sample was needed. A library containing the input DNA (no IP) was constructed. The quantity, size distribution, and purity of the libraries were qualified using a Qubit fluorometer and an Agilent 2100 Bioanalyzer. Sequencing was performed by an Illumina HiSeq X Ten platform (Novogene, Beijing, China). Approximately 30 million reads per sample were obtained.

2.3.3. ChIP-seq data analysis and gene ontology

Quality control was performed using the Saicheng Biology (Guangzhou, China) Sequencing Core with the ENCODE chip pipeline (version 1.8.4). The rattus norvegicus genome version (Rnor 6.0/rn6) was used for mapping with BWA (version 0.7.10). Peaks of enriched H3ac compared to the background input were identified using MACS2 (*41*). BedTools (version 2.27.0) was used to manipulate basic genomic regions, encompassing intersections, and windows (*42*). The enriched peaks were annotated using ChIPpeakAnno (*43*) and ChIPseeker (*44*) based on the rat genome. The promoter regions were determined to be – 3 kb to + 3 kb from the position of the transcription start site (TSS). The differential H3ac modified regions were determined as described previously (*45,46*). In brief, after H3ac regions were confirmed by BedTools (version 2.27.0), the number of reads in those regions was normalized with peaks within 3 kb. The signal was calculated using the IP sample reads per kilobase per million mapped reads (RPKM) minus the input RPKM. As a result, peaks indicating an increase of over 2-fold or a decrease of more than 1/2 between the rats of different ages were defined as differential H3ac regions. The regions enriched with H3ac were identified using the Integrated Genome Viewer (IGV) in alignment with the mapped reads.

2.3.4. qPCR detection of chromatin immunoprecipitated DNA

ChIP-seq data were validated with ChIP-qPCR. The input DNA sample was used for normalization. Primers were selected within the H3Ac-enriched regions detected using ChIP-seq (Table S1, *http://www.biosciencetrends.com/action/getSupplementalData.php?ID=122*). Primers from non-H3Ac region were used as the negative control. Real-time qPCR was performed in triplicate using SYBR Premix Ex Taq (Takara Biomedical Technology, Japan). The relative amount of each amplified fragment was evaluated according to the amplification acquired from input DNA.

2.3.5. RNA extraction and RT-qPCR

The Neasy lipid minikit (Qiagen) was used to purify DNA-free total RNA. The high-capacity cDNA RT kit with ribonuclease inhibitor (Applied Biosystems) was used to perform RT-qPCR. Gene expression was detected with quantitative PCR using the Lightcycle Roche 480 SYBR green master mix (Roche) and the Applied Biosystem 7700 Real-time PCR cycler. With GAPDH as a normalizer, the quantity of the amplified transcripts was calculated using the comparative threshold cycle method. The mean CT values and the ΔΔCT were calculated for duplicate samples. The primer sequences are shown in Table S1 (*http://www.biosciencetrends.com/action/getSupplementalData.php?ID=122*).

2.4. Cell culture

The GT1-7 cell line was cultured in Dulbecco's modified Eagle's medium (DMEM; Life Technologies) containing 10% (vol/vol) FBS (Invitrogen), 100 U/mL penicillin, and 100 μg/mL streptomycin (Sigma-Aldrich) at 37°C in 5% (vol/vol) CO_2. Cells were cultured in media replenished with 10% dextran and charcoal-stripped serum 24 h before treatment. Cells were exposed to E2 (10 mol) or not exposed for 48 h and then exposed to trichostatin A (TSA) (Sigma-Aldrich) at 200 nM for 24 h. Control wells were processed in parallel with the vehicle.

2.5. Drug administration

For LH measurements, TSA (Sigma-Aldrich) was dissolved in 5% dimethyl sulfoxide (DMSO) in saline

to a concentration of 50 ng/mL, 200 ng/mL, or 500 ng/mL. On the day of infusion, middle-aged rats received an icv infusion into the third ventricle *via* microliter syringe (RWD Life Science, China) attached with a plastic connector. The effect of TSA (500 ng/mL) on H3ac was observed in AVPV cells. This concentration was chosen based on its efficacy on LH release. E2 was purchased from Hangxiang Inc. (Wuhan, China) and prepared as previously described (*5*).

2.6. Combined fluorescence in situ hybridization (FISH) and immunohistochemistry

OVX animals were treated with E2 and P and sacrificed during the LH surge as previously described (*39,40*). Blood was collected, and animals were decapitated. The brain was instantly removed, cryopreserved on dry ice, and stored at -80°C until cryogenic sectioning. Brains were coronally cut into five sets of 20-μm sections, thaw-mounted onto Superfrost-plus slides, and stored at -80°C. One set was used for a combined FISH and immunohistochemistry assay.

After fixation in 4% paraformaldehyde, elution in 0.1 M phosphate buffer (pH 7.0), and immersion in proteinase K (20 μg/mL) for 5 min, slide-mounted sections were then placed in prehybridization buffer for 1 h and then with Fam-labeled sense and antisense RNA probes specific to the *Kiss1* sequence (sequences of probes are listed in Table S1, *http://www.biosciencetrends.com/action/getSupplementalData.php?ID=122*). Subsequently, the hybridized sections were rinsed with 2 × SSC, 1 × SSC and 0.5 × SSC, blocked with 1% bovine serum albumin in PBS with 0.25% TritonX-100 for 30 min, incubated overnight with rabbit anti-acetylated histone H3 (AcH3, 1:1200, Millipore) and rabbit anti-c-Fos (1:100, Servicebio) antibodies in blocking solution, and washed in PBS. After incubation with FITC anti-rabbit secondary antibody and counter staining with DAPI, the sections were mounted with anti-fluorescence quenching sealing tablets.

2.7. 3C assay

A 3C assay was performed as in previous studies (37) with some modifications. After 600 U of Kpnl (Roche) was digested, crosslinked chromatin was incubated overnight at 37°C. It was then ligated in 6 mL of 1 × ligation buffer. The *Kiss1* locus encompasses four Kpnl sites; the primers flanking the Kpnl sites were designated K1F: CATGCCAGGTTATACCC CAAC, K1R: CAGAAGTCTGGATCACCAAC, K2F: CTGTG TCATGAGGACGTG, K2R: GGTTCCCGTGATGAAG TAG, K3F: GTGAGAAGAAGACA CTCGTG, K3R: C TGGTGTTATAGCACGTTG, and K-anchor-F: CTGGTGTTATAGCACG TTG. The chromatin loop of the *Kiss1* gene was detected using the primer K-anchor F along with one of the other primers. A loading control region was amplified with CAGGACTGAGGGACGGAAG and GCATCCCTGCC CTGCAAAC. The PCR workflow was as follows: 95°C for 5 min; 35 cycles of 95°C for 30 s, 60°C for 1 min, 72°C for 1 min; and final extension at 72°C for 10 min. The PCR products were detected using agarose gel electrophoresis.

2.8. LH assay

Samples of trunk blood were obtained between 3 P.M. and 5:30 P.M. on the expected day of an LH surge. Serum LH was measured using enzyme-linked immunosorbent assay (ELISA) while LH reagents were provided by the Beijing Sino-UK Institute of Biological Technology (Chaoyang, Beijing).

2.9. Statistical processing

Statistical analyses were performed using the software GraphPad Prism 9.0. Data are expressed as the mean ± SEM. The *t-test* was used to detect differences in the $H3ac^+$ and c-Fos^+ Kiss1 cells in the AVPV and gene expression between groups. Analysis of variance (ANOVA) was used to evaluate the effects of TSA on the *Kiss1* mRNA expression in GT1-7 cells and LH release. Bonferroni or Tukey's post-hoc test was used to identify individual group differences following ANOVA.

3. Results

3.1. Genome-wide ChIP-seq analyses revealed age-associated epigenomic changes in the rat AVPV

Cells containing acetylated histone H3 decreased in the AVPV of middle-aged females as previously reported (*28*), but the total histone H3 did not change (Figure S1 and S2, *http://www.biosciencetrends.com/action/getSupplementalData.php?ID=122*). ChIP-seq was performed to generate a genome-wide landscape of H3ac in the AVPV for OVX middle-aged and young rats that were exposed to E2-positive feedback (Figure 1A). Peak calling analysis was performed using a model-based analysis for ChIP-seq with a false discovery rate (FDR) < 0.05. In total, 91,708 and 143,186 H3ac peaks were identified in middle-aged and young rats, respectively. As shown in Figure 1B, H3ac signals peaked within ± 3 kb from the TSS in both groups.

The feature sets spanning sub-types were defined by genomic locations (Figure 1C) according to the description in the ChIPseeker (*44*): promoter (within ± 3 kb region from the TSS), exon, intron, downstream (3 kb downstream of the transcription termination site, TTS), untranslated region (UTR), and distal intergenic region. Most H3ac modification regions were distributed in the proximal promoter region (≤ 3 kb) and distal intergenic regions. Redistribution to both of the TSSes (≤ 3 kb)

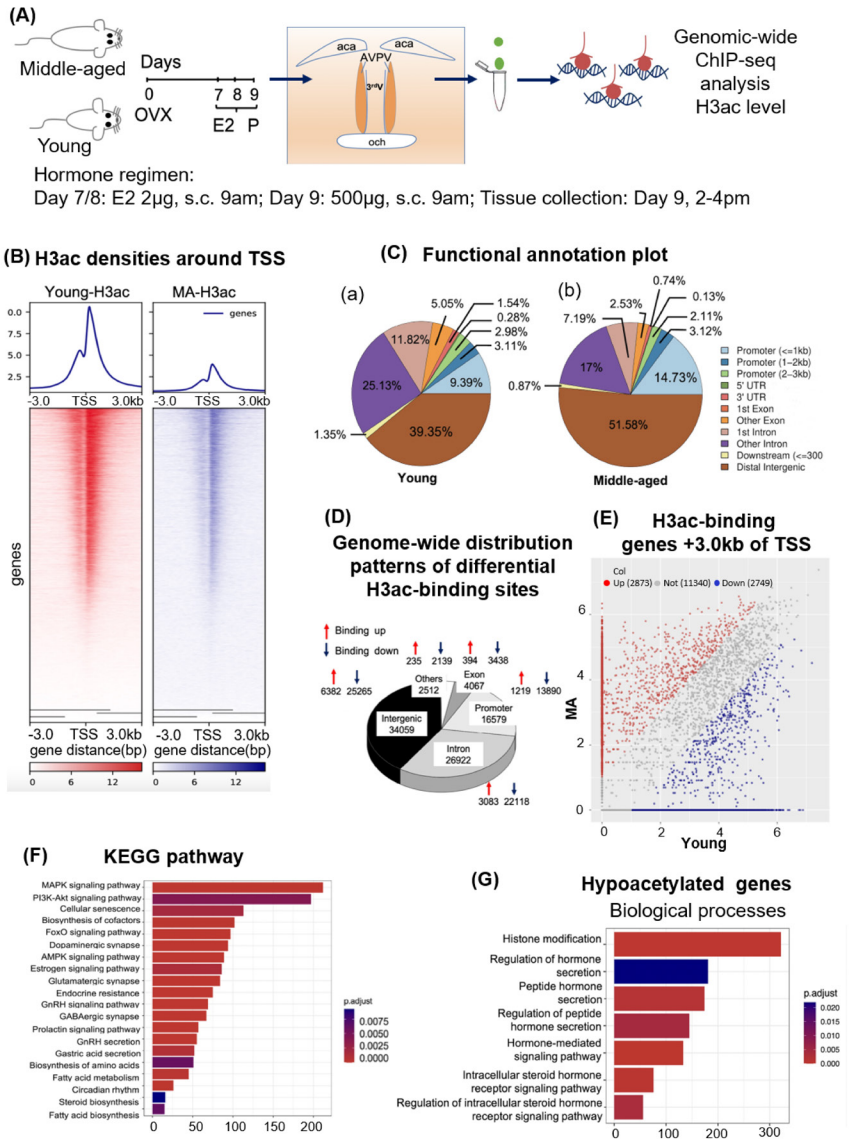

Figure 1. Preponderance of hypoacetylations in the AVPV of middle-aged females compared to young controls and the biological process of hypoacetylated genes under E2 positive feedback. (A) Schematic illustration of the experimental design. Chromatin immunoprecipitation was performed in the AVPV of E2-primed middle-aged and young rats, followed by next-generation sequencing (ChIP-seq). **(B)** Profiles of the active genes (H3ac enrichment) around the TSS. Heatmap showing the H3ac signal from 3 kb upstream to 3 kb downstream of H3ac peaks in middle-aged and young females after normalization. **(C)** Functional annotation plot showing the age-related differential proportion of H3ac regions with several genomic features. **(D)** Pie chart showing the genome-wide distribution patterns of differential H3ac-binding sites in the AVPV in the middle-aged and young groups. Arrows represent sites displaying a significant E2-induced increase (red) or decrease (blue) in H3ac binding. **(E)** The H3ac-binding gene expression pattern in the AVPV of middle-aged and young rats around + 3.0 kb of the TSS. The difference in counts between groups was evaluated using the scatter plot of log2 (RPKM). Red and blue dots represent 3.0 kb upstream of the TSS with different hypoacetylated or hyperacetylated signals in the AVPV of middle-aged animals compared to the controls, while grey dots correspond to unchanged H3ac modification in the AVPV. **(F and G)** Functional enrichment analysis performed with DAVID on the genes associated with hypoacetylated regions were compared in middle-aged and young rats. GO biological processes and KEGG pathways related to histone modification and hormone secretion are shown. The significance is indicated as the log10 *P* value.

and remote intergenic regions was noted in middle-aged females (Figure 1C). Peaks with an increase of over 2-fold or a decrease of more than 1/2 between middle-aged and young females were subsequently defined as differential H3ac regions. As shown in Figure 1D, the H3ac-binding signals markedly decreased in middle-aged rats, and most of the peaks found in the promoter, intergenic, and intron regions were 13,890, 25,265 and 22,118, respectively. The H3ac-binding up regions located in those regions were 1219, 6382 and 3083, respectively.

Most of the H3ac-binding down regions were enriched within ± 3 kb from the TSS (Figure 1B), so the differentially H3ac-associated genes between the two groups were assessed (Figure 1E), and a scatter plot of log2 (RPKM) was prepared. Two thousand eight hundred and seventy-three genes were identified as down-

regulated (16.9%) in the AVPV of middle-aged rats, 2,749 genes were up-regulated (16.2%), and the expression of 11,340 genes did not change (66.9%) (Figure 1E).

Gene ontology (GO) term enrichment analysis was subsequently performed and revealed distinct functional categories for the H3ac-associated gene lists. Within the category of biological processes of the hypoacetylated genes, histone modification and the regulation of hormone secretion were listed as related functions (Figure 1G). Regarding the Kyoto Encyclopedia of Genes and Genomes (KEGG) pathways, the hypoacetylated genes were participants in the mitogen-activated protein kinase (MAPK), neurotransmitter, and hormone signaling pathways (Figure 1F). The top 20 significantly downregulated genes and pathways are shown in Figures S3 and S4 (*http://www.biosciencetrends.com/action/getSupplementalData.php?ID=122*).

3.2. Histone H3 hypoacetylation in the loci of *Kiss1* and *Per1* genes in middle-aged rats

A genome-wide view shows that impaired H3ac in middle-aged females occurred quite homogenously across all chromosomes (Figure 2A). Moreover, hypoacetylated H3 was evaluated in the loci of the pivotal genes involved in the GnRH-LH surge such as *Kiss1* and circadian clock genes with functional histone modification including *Per1*, *Per2*, *Bmal1*, and *Clock* in the AVPV of middle-aged rats (for a representative Integrative Genome Viewer view, see Figure 2B). This finding was confirmed using ChIP followed by qPCR to show that hypoacetylated histone H3 is associated with a significant reduction in *Kiss1*, *Per1*, and *Per2* mRNA (Figure 2C) in middle-aged rats. Consistent with these findings, a 2-fold decrease in *Kiss1* and a 1.5-fold decrease in *Per1* was revealed by qPCR validation analysis versus young controls (Figure 2D, $P < 0.05$, respectively). ChIP-qPCR using primers from non-H3Ac regions revealed no significant differences (data not shown). Overall, these experiments identified several genes associated with the hormone-mediated LH surge and reproductive regulation and with the altered H3ac profile in the AVPV of middle-aged females undergoing a reproductive decline.

3.3. Suppressed H3ac in AVPV Kiss1 cells is associated with attenuated *Kiss1* transcriptional activation in middle-aged rats

FISH and immunofluorescence revealed that the cells expressing *Kiss1* mRNA were abundant in the AVPV (Figure 3A), but few of them were H3ac^{+} in young and middle-aged OVX rats (Figure 3A-a and g). In line with a previous study (*28*), the AVPV from young females

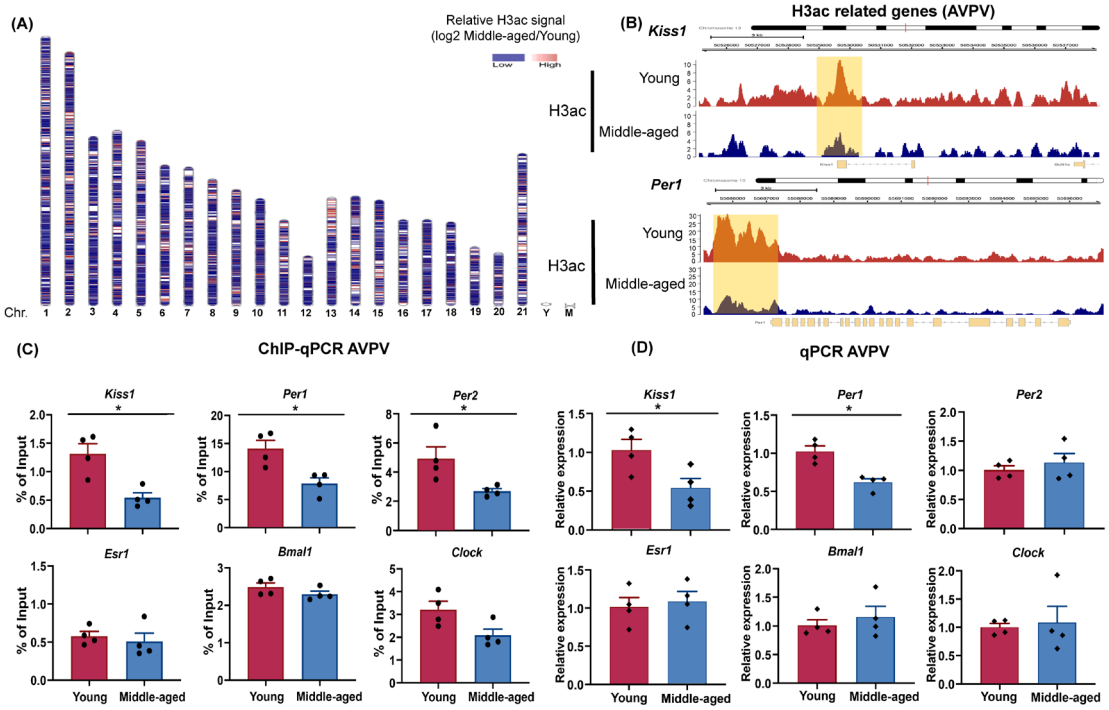

Figure 2. Altered chromosomal distribution of H3ac reads and acetylation signatures in the AVPV of middle-aged rats. (A) Chromosome ideogram showing the level of H3ac peaks across the chromosomes of middle-aged female rats compared to young female rats. The color key from blue to red indicates low to high relative levels of H3ac, respectively. **(B)** Representative tracks of *Kiss1* and *Per1* ChIP-seq data showing pronounced loss of the H3ac signal in the AVPV of middle-aged rats. **(C)** Chromatin was isolated from the AVPV removed from middle-aged ($n = 4$) and young ($n = 4$) females. ChIP-qPCR experiments performed in the two groups of animals. Unpaired Mann-Whitney *t-test*. **(D)** qRT-PCR analyses using primers against the genes listed were performed in AVPV tissues of young ($n = 4$) and middle-aged offspring ($n = 4$). Unpaired Mann-Whitney *t-test*. Data in **(C)** and **(D)** are expressed as the mean ± SEM. $^{*}P < 0.05$.

primed with E2 exhibited a marked increase in H3ac immunoreactivity and H3ac^{+} was strikingly identified within Kiss1 cells. Detailed quantification subsequently revealed that approximately 42% of *Kiss1*-expressing cells located in the AVPV were H3ac^{+} ($P < 0.001$, Figure 3A-f and l). However, H3ac^{+} induced in AVPV Kiss1 cells by E2 was disrupted to approximately 24% in middle-aged females (Figure 3A-l and o, $P < 0.001$). The percentage of H3ac^{+} Kiss1 cells decreased markedly by approximately 60% compared to that in young controls treated with E2.

Given the close association between histone acetylation and chromatin accessibility and the transcriptional activity of cells (*20,36,47*), whether the suppressed H3ac in AVPV Kiss1 cells observed in middle-aged females (Figure 3A-l and o) was associated with a parallel decline in *Kiss1* transcriptional activation was determined next. C-Fos immunoreactivity was used as a marker for Kiss1 neuronal activation in the AVPV (Figure 3B) based on previous studies by the current authors (*39,40*). Approximately 32% of AVPV Kiss1 cells from E2-primed young females had c-Fos^{+} nuclei (Figure 3B-a and c). FISH and IF profiles revealed marked impairment in c-Fos immunoreactivity in middle-aged rats (Figure 3B-d, $P < 0.05$); that is, the percentage of c-Fos^{+} Kiss1 cells decreased to approximately 20% (Figure 3B-b and c, $P < 0.05$).

3.4. TSA promotes *Kiss1* transcription and counteracts neuroendocrine dysfunction in middle-aged females by enhancing H3ac

ChIP-seq analyses pointed to a preponderance of hypoacetylation in the AVPV of middle-aged rats, so the therapeutic potential of TSA was examined next (Figure 4). The effects of TSA on *Kiss1* expression in GT1-7 cells were first tested using a mouse-derived immortalized GnRH-secreting neuronal cell line (Figure 4A-a). E2 exposure (10 mol) induced a significant 20-fold increase in *Kiss1* expression in the cell line. *Kiss1* mRNA increased significantly in GT1-7 cells as a result of TSA (200 nmol). Moreover, the level was strikingly upregulated by the simultaneous presence of both TSA and E2 (Figure 4A-b). Thereafter, cycling middle-aged

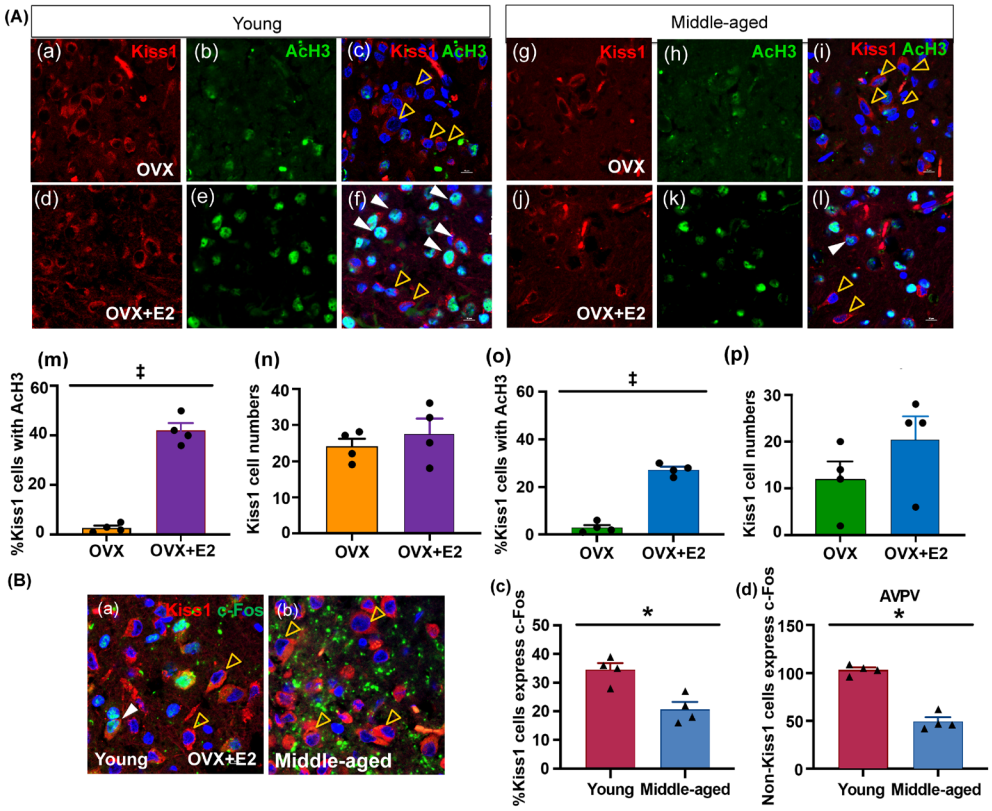

Figure 3. Middle-aged female rats exhibit suppressed histone H3ac in Kiss1^{AVPV} associated with reduced c-Fos expression. (A) Confocal representative photomicrographs showing *Kiss1* and H3ac immunoreactivity in the AVPV. 3V, third ventricle. Bars, 10 μm. **(a–f)** and **(g-l)** Kiss1^{AVPV} cells with (white solid triangles) or without H3ac (yellow open triangles) in young and middle-aged rats primed with E2 or oil, as determined by FISH combined with IF (*Kiss1* mRNA, red; H3ac, green). **(m-n)** and **(o-p)** Quantitative analysis of the percentage of H3ac^{+} Kiss1^{AVPV} cells in young ($n = 4$) and middle-aged females ($n = 4$) after E2 or oil treatment. **(B)** C-Fos^{+} Kiss1 neurons decreased in the AVPV of middle-aged females treated with E2. **(a)** Representative AVPV section showing Kiss1 cells expressing c-Fos in young rats. **(b)** Kiss1 cells lack activation to express c-Fos in middle-aged rats. **(c)** and **(d)** Statistical analysis of c-Fos expression in Kiss1 and non-Kiss1 cells in the AVPV of young and middle-aged rats. Bars, 100 μm. The statistical significance for all analyses was $^{*}P < 0.05$; $^{‡}P < 0.001$.

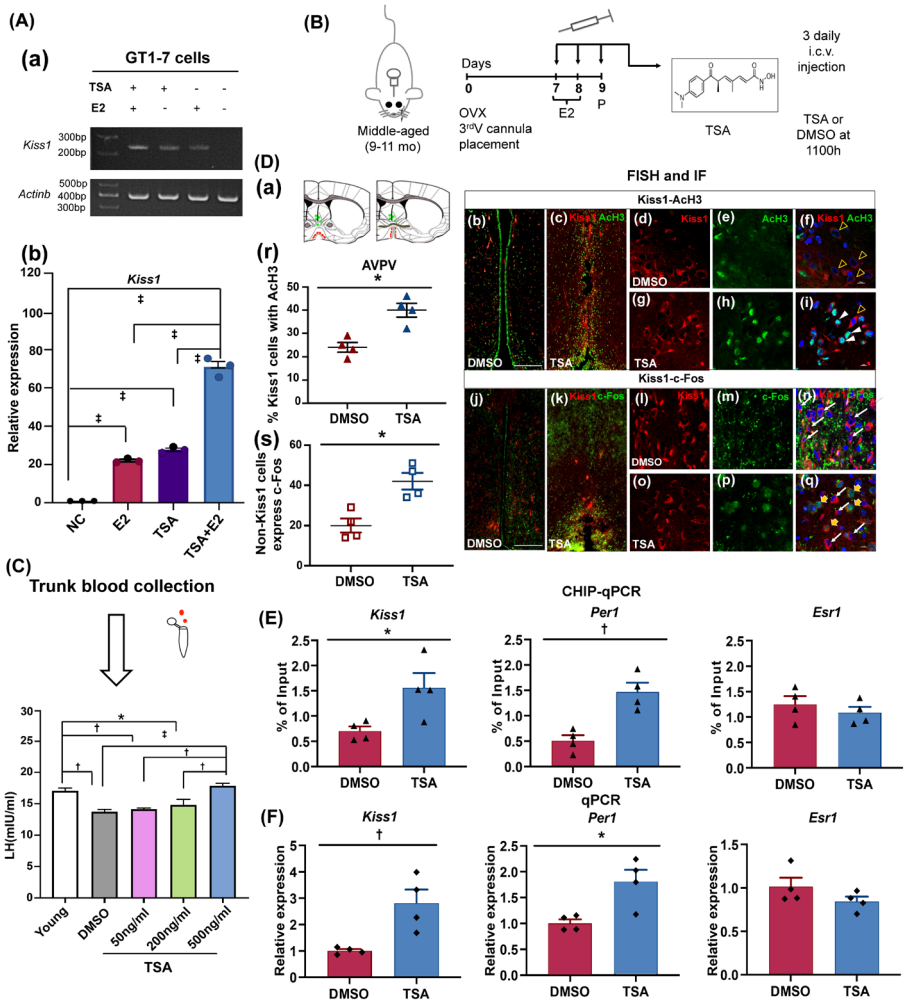

Figure 4. Histone deacetylase inhibitor TSA rescues neuroendocrine dysfunction in middle-aged females by modulating hypoacetylated genes in the AVPV. (A) Effects of inhibitors of histone deacetylation on *Kiss1* expression in the immortalized GT1-7 cell line. RT-PCR analysis of *Kiss1* gene expression in GT1-7 cells treated with 200 nM of TSA. **(B)** Schematic illustration of the experimental design. TSA or DMSO was injected into the third cerebral ventricle of middle-aged rats treated with E2. **(C)** Mean LH levels were measured using trunk blood collected from middle-aged (3-4 h after TSA or DMSO injection) and young rats treated with E2. **(D)** Icv injection of TSA enhances H3ac and improves c-Fos expression in Kiss1^{AVPV}. **(a)** Brain sections of the hypothalamic AVPV were collected. **(b-i)** Representative FISH combined with IF images showing H3ac or non-H3ac in Kiss1^{AVPV} after TSA or DMSO treatment. **(j-q)** Representative FISH combined with IF pictures showing c-Fos or non-c-Fos expressed Kiss1^{AVPV} cells in the groups treated with TSA or DMSO. **(r)** Quantitative analysis of the percentage of H3ac^{+} in Kiss1^{AVPV} cells in the groups treated with TSA (n = 4) or DMSO (n = 4). **(s)** Quantitative analysis of the percentage of Kiss1^{AVPV} cells expressing c-Fos in the groups treated with TSA (n = 4) or DMSO (n = 4). **(E)** and **(F)** Statistical analysis of ChIP-qPCR and qPCR data on young and middle-aged rats treated with TSA or DMSO (n = 4, respectively). The statistical significance for all analyses was $^{*}P < 0.05$; $^{\dagger}P < 0.01$; $^{\ddagger}P < 0.001$.

rats were selected and treated with daily icv injections of DMSO or different doses of TSA (Figure 4B). Trunk blood samples were collected upon sacrifice of the rats for LH measurement on the predicted day of an LH surge. Control animals had a high level of LH release, while 500 ng/mL of TSA restored LH release compared to that in females treated with DMSO ($P < 0.001$, Figure 4C).

Next, whether TSA had a directly effect on Kiss1 neurons was examined. In line with previous data (see Figure 3A), there were few H3ac^{+} Kiss1 neurons in middle-aged rats treated with DMSO (Figure 4D-b and f). The TSA treatment significantly induced a 1.5-fold increase in H3ac^{+} Kiss1 cells in the AVPV ($P < 0.05$, Figure 4D-c, i and r). Similarly, rats treated with TSA had a marked increase in the c-Fos^{+} nuclei of the AVPV Kiss1 cells by approximately 50% compared to that in rats treated with DMSO ($P < 0.05$, Figure 4D-k, q and s). Whether LH restored by TSA (Figure 4C) was associated with an epigenetic effect of H3ac was also determined. ChIP-qPCR assays were performed to target the different gene loci of *Kiss1*, *Per1*, and *Esr1*. A marked increase in H3ac was observed in the enhancer region of *Kiss1* ($P < 0.05$) and in the promoter region of *Per1* as a result of TSA ($P < 0.01$). Changes in H3ac were not observed at *Esr1* (Figure 4E).

To further evaluate the effect of TSA on the levels of gene expression, qRT-PCR of *Kiss1*, *Per1*, and *Esr1* was performed (Figure 4F). Levels of *Esr1* transcription were comparable among the different groups, but *Kiss1*

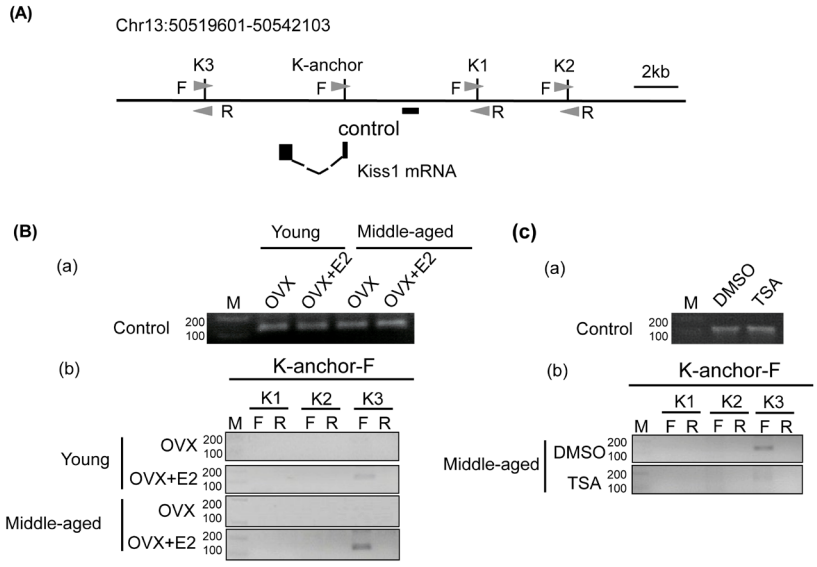

Figure 5. Icv administration of TSA modifies chromatin loop formation at the *Kiss1* gene locus in the AVPV of middle-aged rats. (A) Diagram of the *Kiss1* locus; filled boxes indicate exons, and thin dotted lines indicate introns. Kpnl restriction endonuclease sites are indicated by vertical lines (labeled as K1–K3). Arrows show the positions of primers used in 3C assays. The thick horizontal bar indicates the region used in loading control PCR. **(B)** Chromatin loop formation at the *Kiss1* gene locus in the AVPV of middle-aged rats. **(a)** PCR for loading control. Tissue from the AVPV was sampled in young and middle-aged OVX rats with (OVX+E2) or without E2 treatment (OVX). **(b)** 3C analysis of the *Kiss1* locus obtained from AVPV tissue from young and middle-aged females exposed or not exposed to E2. 3C assays were performed, and the PCR products were analyzed using agarose gel electrophoresis. The PCR products were generated using the primer K-anchor forward (K-anchor-F) along with one of the other Kpnl primers (K1–K3) as indicated. **(C)** TSA induces chromatin conformational loop changes at the *Kiss1* gene locus in the AVPV of middle-aged rats. **(a)** PCR for loading control. Tissue from the AVPV was sampled from OVX+E2-primed middle-aged rats injected with TSA or DMSO. **(b)** PCR products of a 3C assay were analyzed using agarose gel electrophoresis. Primers and PCR products were generated as described above.

and *Per1* were significantly upregulated in the group treated with TSA (Figure 4F; $P < 0.01$ and $P < 0.05$, respectively).

3.5. The mechanism of reduced *Kiss1* gene expression in middle-age includes changes in chromatin looping associated with histone hypoacetylation

Chromatin access (opening) to transactivating factors driven by histone acetylation is the major epigenetic mechanism for gene transcription (*47*). Whether the chromatin conformational loop changed at the AVPV *Kiss1* gene loci after E2 treatment was assessed using 3C primers as shown in Figure 5A. The intensity of PCR products for the controls did not differ between the groups (Figure 5B-a). No PCR products were observed with the K2F-K1R, K3F-K1R, and K1F-K2R primers in the OVX young or middle-aged groups ($n = 4$, Figure 5B-b), indicating that there were no looping interactions without E2. E2 treatment increased the 3′ PCR products with K-anchor-K3F primers (Figure 5B-b) in the AVPV of young rats. These results indicate that chromatin loop formation between the promoter and the 3' intergenic region of *Kiss1* is enhanced by E2. The patterns of chromatin loop formation within the *Kiss1* loci differ between young and middle-aged rats. The PCR product obtained using primers between the promoter and 3′ intergenic region markedly increased in the rats, suggesting that an intense loop was formed in the 3′ region under E2-positive feedback conditions (Figure 5B-b). Whether H3ac drove the differential chromatin looping conformation of the AVPV *Kiss1* gene was further examined in middle-aged females using TSA. PCR products of the 3C assay with the K-anchor-K3F primer sets displayed less intensity. The intensity of the PCR product decreased to a level similar to that in young females treated with E2 (Figure 5C-b), indicating that H3ac enhancement by TSA normalized loop formation in the 3′ intergenic region, which in turn permitted *Kiss1* transcription. There were no differences in the amounts of PCR products for the controls among the groups (Figure 5C-a).

4. Discussion

The current study has provided the first high-throughput sequencing profile of epigenome changes in the AVPV. This key E2-positive feedback region is causally involved in neuroendocrine impairment in female reproductive aging. Given the importance of the hyperacetylation of histones in the promoter region to gene expression induced by steroid hormones (*24,35,48,49*), advanced reproductive age heavily contributed to differential H3ac peaks enriched by the TSS in the AVPV; a preponderance of hypoacetylation in particular contributed to the altered gene expression in middle-aged females under E2-

positive feedback conditions. This conclusion is backed up by AVPV ChIP-seq data showing the hypoacetylation of histone H3 coupled with changes in the expression of 33.1% of genes. Despite the number of sequences and regions involved in histone acetylation and the complex chromatin alterations that exist alongside gene expression (*10*), the current data expand our understanding that age-dependent epigenomic changes ultimately defining the AVPV cellular transcriptional response to E2 may cause the dysregulation of transcriptional and chromatin networks in advanced age. Interestingly, GO and KEGG analyses revealed that age-related differences in histone acetylation occurring in specific genes and pathways were associated with reproduction and hormone secretion as well as neurotransmitter synapses. The selective analysis of epigenomic changes in several neuronal and non-neuronal cells using genetic strategies such as the fluorescently tagged technique combined with fluorescence activated nuclear sorting (FANS) to isolate specific cell types from the AVPV would further increase our understanding of aging GnRH neuronal networks.

Tomikawa *et al.* found that increased E2-promoted H3ac and ERα binding in the promoter region of *Kiss1*^{AVPV} positively enhanced *Kiss1* gene expression (*35*), suggesting that the promoter region is critical to E2-activated *Kiss1* gene expression. Bioinformatic analysis predicted that a reduction in *Kiss1* in the AVPV of middle-aged rats was the result of the hypoacetylation of histone H3 at the 3′ intergenic region of the *Kiss1* loci. Removal of the 3' region, which is known to be a functional estrogen-responsive enhancer for *Kiss1*, in Tg-2 mice reduced GFP expression induced by estrogen in *Kiss1* (*35*). The acetylation of histones changes the chromatin flexibility in the nucleus and the interaction between the coding gene and its remote enhancer, but a low acetylation threshold destabilizes higher-order folding, which has a similar effect to N-terminal removal (*21,50*). Therefore, suppressed H3ac in the 3′ region of *Kiss1* may weaken its facilitating role in chromatin-looping conformation for *Kiss1* transcription. As indicated by the 3C assay, the interaction between the promoter and 3′ region of *Kiss1 via* chromatin looping is likely to be associated with E2-dependent *Kiss1* expression in the AVPV of young females. H3ac decreased markedly in middle-aged rats, but an intensified chromatin loop between the promoter and 3′ region of *Kiss1* was notably detected and was associated with reduced *Kiss1* expression. These discordant findings can be explained by the 3′ enhancer region of *Kiss1*, which may be a specific locus that loses sensitivity to E2 when females transition to middle age, or by the hypoacetylation of histone H3, which is continuously responsible for looping conformation but which finally changes chromatin to an "off" state. Nevertheless, age-associated changes in H3ac may induce a stable repressive higher-order chromatin structure *via* a CCCTC binding factor (CTCF) in the AVPV nuclei of middled-aged animals to suppress gene expression despite E2 positive feedback.

The current study also found that expression of a circadian gene, *Per1*, was affected by the hypoacetylation of histone H3. Previous studies have reported the circadian regulation of higher-order chromatin formation (*37*), long-range interchromosomal interplay (*51*), and short-range looping at specific loci (*52,53*). AVPV *Kiss1* cells express *Per1* with an E2-sensitive circadian rhythm (*54,55*); however, whether the H3ac-mediated suppression of *Per1* ultimately limited *Kiss1* expression remains unknown. Evaluating the complex dynamics between *Per1*, *Kiss1*, and other molecular players is an important topic of future research.

Even more strikingly, the current results revealed that the administration of TSA to E2-primed middle-aged rats corrected neuroendocrine alterations and rescued GnRH/LH release. Consistent with previous studies which found that TSA intensified the transcription of the *c-fos* and *c-jun* genes in neurons after kainite stimulation (*56*), TSA significantly increased c-Fos activation in the Kiss1 cells of middle-aged females, suggesting an appropriate level of histone acetylation is required to activate *Kiss1* transcription. The current findings are also consistent with those of a recent study which found that histone hyperacetylation induced by TSA can induce *Kiss1* expression in the mouse hypothalamic cell line N6 (*35*), suggesting that reduced H3ac may result in negative down-stream effects on GnRH neuron activation and LH release. An HDAC inhibitor is clinically used for cancer treatment (*57-59*). The current study cannot rule out the possibility that TSA promoted some other gene expression or protein acetylation in the GnRH neuronal network, but the current results highlight the therapeutic potential of acetylation agents as promising epigenetic therapies to treat women with LH surge dysfunction.

Under E2 positive feedback, *Esr1* is required for E2-regulated gene expression in the hypothalamus (*6,60*). Acetylation of the *Esr1* hinge region manipulates transcriptional transactivation and hormone sensitivity (*61*), but the level of H3ac at the *Esr1* promoter and the *Esr1* mRNA in middle-aged females is similar to that in young females. These data do not support the contention that decreased H3ac at the regulatory sequences of *Esr1* reduces *Kiss1* expression in the AVPV of middle-aged females.

In summary, the current study provides evidence showing that altered H3ac plays a pivotal role in age-related neuroendocrine changes, including LH disorders. That said, specific histone H3 lysine acetylation remains to be determined. Other epigenetic modifications cannot be excluded as contributing factors, but recent studies have confirmed the unique role of H3ac in orchestrating E2-induced gene expression under positive feedback. Therefore, H3ac seems to be of particular importance to transcriptional activation as characterized by hyperacetylation along gene bodies. In addition, the

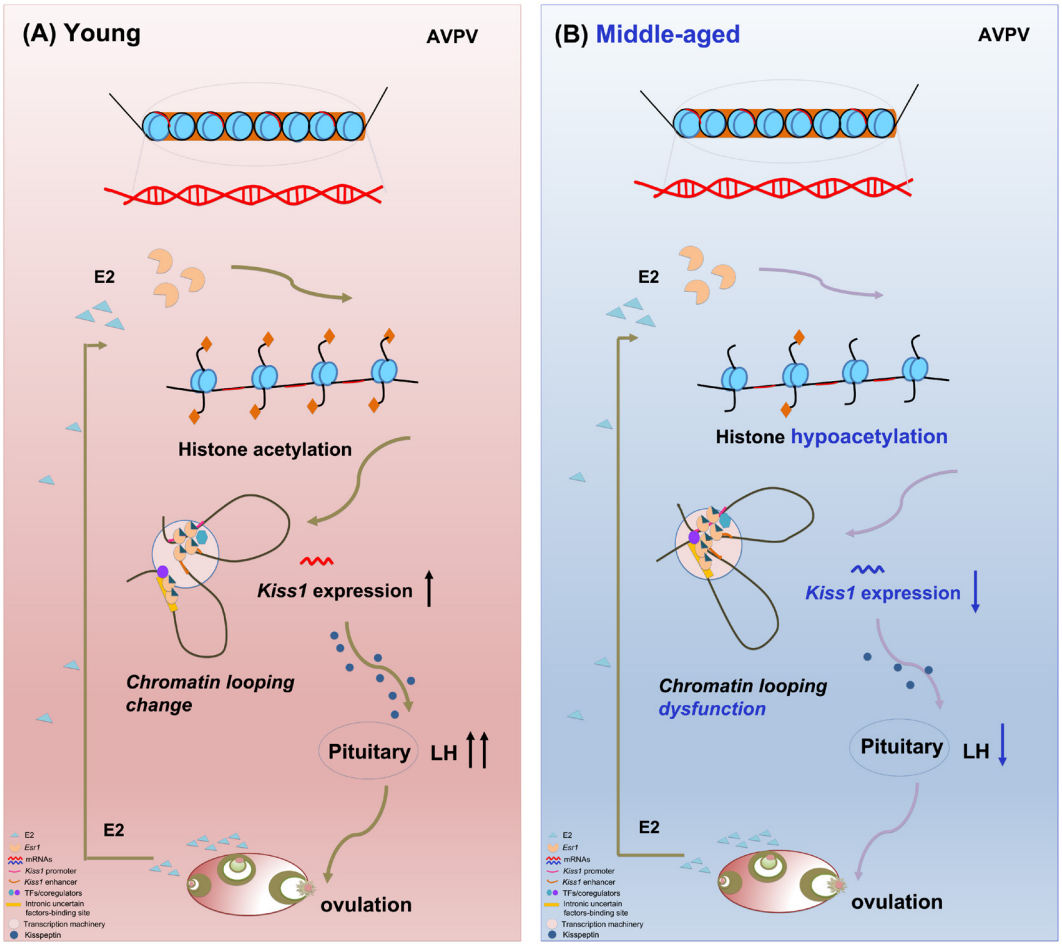

Figure 6 Schematic representation of the proposed mechanism of epigenomic alterations modifying the expression of genes such as *Kiss1* in the rat AVPV to control female reproductive aging. This diagram shows possible epigenomic regulation of gene expression in the AVPV under E2-positive feedback conditions. **(A)** In young females, the E2-ESR1 complex induces histone H3ac and opens the chromatin structure, consequently enhancing the formation of a chromatin loop between the *Kiss1* promoter and the 3′ enhancer region, promoting transcription. **(B)** In middle-aged females, decreased histone H3 acetylation associated with an altered chromatin state may cause transcriptional inaction by formatting the inhibitory chromatin loop between the *Kiss1* promoter and the 3′ enhancer region.

dysregulation of H3ac in middle age is mainly found along with reduced gene expression. Altered H3ac may manipulate *Kiss1* expression in particular by remodeling chromatin (Figure 6). This work presents important insights into the molecular mechanisms underlying reduced responsiveness to E2-positive feedback in specific regions of the hypothalamus when females transition into perimenopause.

Acknowledgements

The authors wish to sincerely thank Peng Li and Suna Tian for their assistance in preparing the figures in this manuscript.

Funding: This research was supported by the Shanghai Natural Science Foundation (grant no.17ZR1403300 to Y Sun), the National Natural Science Foundation of China for Young Investigators (grant no. 31800987 to Y Sun) and the National Natural Science Foundation of China (grant no. 82074531 to Y Sun), a project under the Scientific and Technological Innovation Action Plan of the Shanghai Natural Science Fund (grant no. 20ZR1409100 to L Wang), a project of the Chinese Association of Integration of Traditional and Western Medicine special foundation for Obstetrics and Gynecology-PuZheng Pharmaceutical Foundation (grant no. FCK-PZ-08 to L Wang), a project for hospital management of the Shanghai Hospital Association (grant no. X2021046 to L Wang), and a clinical trial project of the Special Foundation for Healthcare Research of the Shanghai Municipal Health Commission (grant No. 202150042 to L Wang).

Conflict of Interest: The authors have no conflicts of interest to disclose.

References

1. Le WW, Wise PM, Murphy AZ, Coolen LM, Hoffman GE. Parallel declines in Fos activation of the medial anteroventral periventricular nucleus and LHRH neurons

in middle-aged rats. Endocrinology. 2001; 142:4976-4982.
2. Kauffman AS, Sun Y, Kim J, Khan AR, Shu J, Neal-Perry G. Vasoactive intestinal peptide modulation of the steroid-induced LH surge involves kisspeptin signaling in young but not in middle-aged female rats. Endocrinology. 2014; 155:2222-2232.
3. Xie Q, Kang Y, Zhang C, Xie Y, Wang C, Liu J, Yu C, Zhao H, Huang D. The role of kisspeptin in the control of the hypothalamic-pituitary-gonadal axis and reproduction. Front Endocrinol (Lausanne). 2022; 13:925206.
4. Austad SN. Sex differences in health and aging: A dialog between the brain and gonad? Geroscience. 2019; 41:267-273.
5. Neal-Perry GS, Zeevalk GD, Santoro NF, Etgen AM. Attenuation of preoptic area glutamate release correlates with reduced luteinizing hormone secretion in middle-aged female rats. Endocrinology. 2005; 146:4331-4339.
6. Chakraborty TR, Hof PR, Ng L, Gore AC. Stereologic analysis of estrogen receptor alpha (ER alpha) expression in rat hypothalamus and its regulation by aging and estrogen. J Comp Neurol. 2003; 466:409-421.
7. Chakraborty TR, Ng L, Gore AC. Age-related changes in estrogen receptor beta in rat hypothalamus: A quantitative analysis. Endocrinology. 2003; 144:4164-4171.
8. Brown TJ, MacLusky NJ, Shanabrough M, Naftolin F. Comparison of age- and sex-related changes in cell nuclear estrogen-binding capacity and progestin receptor induction in the rat brain. Endocrinology. 1990; 126:2965-2972.
9. Engmann O, Labonté B, Mitchell A*, et al.* Cocaine-induced chromatin modifications associate with increased expression and three-dimensional looping of Auts2. Biol Psychiatry. 2017; 82:794-805.
10. Ferrari R, de Llobet Cucalon LI, Di Vona C, Le Dilly F, Vidal E, Lioutas A, Oliete JQ, Jochem L, Cutts E, Dieci G, Vannini A, Teichmann M, de la Luna S, Beato M. TFIIIC binding to Alu elements controls gene expression *via* chromatin looping and histone acetylation. Mol Cell. 2020; 77:475-487.e411.
11. Anderson EM, Taniguchi M. Epigenetic effects of addictive drugs in the nucleus accumbens. Front Mol Neurosci. 2022; 15:828055.
12. Fernandez-Albert J, Lipinski M, Lopez-Cascales MT, Rowley MJ, Martin-Gonzalez AM, Del Blanco B, Corces VG, Barco A. Immediate and deferred epigenomic signatures of *in vivo* neuronal activation in mouse hippocampus. Nat Neurosci. 2019; 22:1718-1730.
13. Bonnaud EM, Suberbielle E, Malnou CE. Histone acetylation in neuronal (dys)function. Biomol Concepts. 2016; 7:103-116.
14. Girdhar K, Hoffman GE, Jiang Y, *et al.* Cell-specific histone modification maps in the human frontal lobe link schizophrenia risk to the neuronal epigenome. Nat Neurosci. 2018; 21:1126-1136.
15. Kubben N, Misteli T. Shared molecular and cellular mechanisms of premature ageing and ageing-associated diseases. Nat Rev Mol Cell Biol. 2017; 18:595-609.
16. Fallah MS, Szarics D, Robson CM, Eubanks JH. Impaired regulation of histone methylation and acetylation underlies specific neurodevelopmental disorders. Front Genet. 2020; 11:613098.
17. Kurdistani SK, Tavazoie S, Grunstein M. Mapping global histone acetylation patterns to gene expression. Cell. 2004; 117:721-733.
18. Shvedunova M, Akhtar A. Modulation of cellular processes by histone and non-histone protein acetylation. Nat Rev Mol Cell Biol. 2022; 23:329-349.
19. Ozawa H. Masterful papers that broke open understanding of reproductive neuroendocrinology. Nat Rev Endocrinol. 2022.
20. Kristjuhan A, Walker J, Suka N, Grunstein M, Roberts D, Cairns BR, Svejstrup JQ. Transcriptional inhibition of genes with severe histone H3 hypoacetylation in the coding region. Mol Cell. 2002; 10:925-933.
21. Li B, Carey M, Workman JL. The role of chromatin during transcription. Cell. 2007; 128:707-719.
22. Yi SJ, Kim K. New insights into the role of histone changes in aging. Int J Mol Sci. 2020; 21.
23. Fan L, Zhao Z, Orr PT, Chambers CH, Lewis MC, Frick KM. Estradiol-induced object memory consolidation in middle-aged female mice requires dorsal hippocampal extracellular signal-regulated kinase and phosphatidylinositol 3-kinase activation. J Neurosci. 2010; 30:4390-4400.
24. Gagnidze K, Weil ZM, Faustino LC, Schaafsma SM, Pfaff DW. Early histone modifications in the ventromedial hypothalamus and preoptic area following oestradiol administration. J Neuroendocrinol. 2013; 25:939-955.
25. Frick KM, Tuscher JJ, Koss WA, Kim J, Taxier LR. Estrogenic regulation of memory consolidation: A look beyond the hippocampus, ovaries, and females. Physiol Behav. 2018; 187:57-66.
26. Kovács T, Szabó-Meleg E, Ábrahám IM. Estradiol-induced epigenetically mediated mechanisms and regulation of gene expression. Int J Mol Sci. 2020; 21.
27. Xu W, An X, Zhang N, Li L, Zhang X, Wang Y, Wang L, Sun Y. Middle-aged female rats lack changes in histone H3 acetylation in the anterior hypothalamus observed in young females on the day of a luteinizing hormone surge. Biosci Trends. 2019; 13:334-341.
28. Xu W, Huang J, Li L, Zhang X, Wang Y, Tong G, Sun Y. Alterations of estradiol-induced histone H3 acetylation in the preoptic area and anteroventral periventricular nucleus of middle-aged female rats. Biochem Biophys Res Commun. 2019; 516:894-899.
29. Xu W, Zhang N, Li LS, Wang Y, Wang L, Du MR, Li DJ, Sun Y. Gene expression pattern of histone acetylation enzymes changed in the hypothalamus of middle-aged female rats: A putative mechanism for female reproductive aging. Reprod Dev Med. 2018; 2:65-73.
30. Uenoyama Y, Inoue N, Nakamura S, Tsukamura H. Kisspeptin neurons and estrogen-estrogen receptor alpha signaling: Unraveling the mystery of steroid feedback system regulating mammalian reproduction. Int J Mol Sci. 2021; 22.
31. Adams C, Stroberg W, DeFazio RA, Schnell S, Moenter SM. Gonadotropin-releasing hormone (GnRH) neuron excitability is regulated by estradiol feedback and kisspeptin. J Neurosci. 2018; 38:1249-1263.
32. Sobrino V, Avendaño MS, Perdices-López C, Jimenez-Puyer M, Tena-Sempere M. Kisspeptins and the neuroendocrine control of reproduction: Recent progress and new frontiers in kisspeptin research. Front Neuroendocrinol. 2022; 65:100977.
33. Kimura M, Ishii MN, Seki N, Sakai Y, Yamashita T, Awatsuji H, Kanda K, Matsumoto K, Matsui H. Reduction of Kiss1 expression in the anteroventral periventricular nucleus is associated with atrazine-induced attenuation of the luteinizing hormone surge in female rats. Biol Reprod. 2019; 100:41-48.
34. Lederman MA, Lebesgue D, Gonzalez VV, Shu J, Merhi

ZO, Etgen AM, Neal-Perry G. Age-related LH surge dysfunction correlates with reduced responsiveness of hypothalamic anteroventral periventricular nucleus kisspeptin neurons to estradiol positive feedback in middle-aged rats. Neuropharmacology. 2010; 58:314-320.
35. Tomikawa J, Uenoyama Y, Ozawa M, *et al.* Epigenetic regulation of Kiss1 gene expression mediating estrogen-positive feedback action in the mouse brain. Proc Natl Acad Sci U S A. 2012; 109:E1294-1301.
36. Semaan SJ, Kauffman AS. Emerging concepts on the epigenetic and transcriptional regulation of the *Kiss1* gene. Int J Dev Neurosci. 2013; 31:452-462.
37. Zhao H, Sifakis EG, Sumida N, *et al.* PARP1- and CTCF-Mediated interactions between active and repressed chromatin at the lamina promote oscillating transcription. Mol Cell. 2015; 59:984-997.
38. Akgol Oksuz B, Yang L, Abraham S, *et al.* Systematic evaluation of chromosome conformation capture assays. Nat Methods. 2021; 18:1046-1055.
39. Sun Y, Todd BJ, Thornton K, Etgen AM, Neal-Perry G. Differential effects of hypothalamic IGF-I on gonadotropin releasing hormone neuronal activation during steroid-induced LH surges in young and middle-aged female rats. Endocrinology. 2011; 152:4276-4287.
40. Sun Y, Shu J, Kyei K, Neal-Perry GS. Intracerebroventricular infusion of vasoactive intestinal peptide rescues the luteinizing hormone surge in middle-aged female rats. Front Endocrinol (Lausanne). 2012; 3:24.
41. Zhang Y, Liu T, Meyer CA, Eeckhoute J, Johnson DS, Bernstein BE, Nusbaum C, Myers RM, Brown M, Li W, Liu XS. Model-based analysis of ChIP-seq (MACS). Genome Biol. 2008; 9:R137.
42. Quinlan AR, Hall IM. BEDTools: A flexible suite of utilities for comparing genomic features. Bioinformatics. 2010; 26:841-842.
43. Zhu LJ, Gazin C, Lawson ND, Pagès H, Lin SM, Lapointe DS, Green MR. ChIPpeakAnno: A bioconductor package to annotate ChIP-seq and ChIP-chip data. BMC Bioinformatics. 2010; 11:237.
44. Yu G, Wang LG, He QY. ChIPseeker: An R/Bioconductor package for ChIP peak annotation, comparison and visualization. Bioinformatics. 2015; 31:2382-2383.
45. Tamura I, Ohkawa Y, Sato T, Suyama M, Jozaki K, Okada M, Lee L, Maekawa R, Asada H, Sato S, Yamagata Y, Tamura H, Sugino N. Genome-wide analysis of histone modifications in human endometrial stromal cells. Mol Endocrinol. 2014; 28:1656-1669.
46. Troutman TD, Kofman E, Glass CK. Exploiting dynamic enhancer landscapes to decode macrophage and microglia phenotypes in health and disease. Mol Cell. 2021; 81:3888-3903.
47. Clayton AL, Hazzalin CA, Mahadevan LC. Enhanced histone acetylation and transcription: A dynamic perspective. Mol Cell. 2006; 23:289-296.
48. Chen H, Lin RJ, Xie W, Wilpitz D, Evans RM. Regulation of hormone-induced histone hyperacetylation and gene activation *via* acetylation of an acetylase. Cell. 1999; 98:675-686.
49. Frick KM, Kim J. Mechanisms underlying the rapid effects of estradiol and progesterone on hippocampal memory consolidation in female rodents. Horm Behav. 2018; 104:100-110.
50. Tse C, Sera T, Wolffe AP, Hansen JC. Disruption of higher-order folding by core histone acetylation dramatically enhances transcription of nucleosomal arrays by RNA polymerase iii. Mol Cell Biol. 1998; 18:4629-4638.
51. Aguilar-Arnal L, Hakim O, Patel VR, Baldi P, Hager GL, Sassone-Corsi P. Cycles in spatial and temporal chromosomal organization driven by the circadian clock. Nat Struct Mol Biol. 2013; 20:1206-1213.
52. Xu Y, Guo W, Li P, Zhang Y, Zhao M, Fan Z, Zhao Z, Yan J. Long-range chromosome interactions mediated by cohesin shape circadian gene expression. PLoS Genet. 2016; 12:e1005992.
53. Furlan-Magaril M, Ando-Kuri M, Arzate-Mejía RG, Morf J, Cairns J, Román-Figueroa A, Tenorio-Hernández L, Poot-Hernández AC, Andrews S, Várnai C, Virk B, Wingett SW, Fraser P. The global and promoter-centric 3D genome organization temporally resolved during a circadian cycle. Genome Biol. 2021; 22:162.
54. Chassard D, Bur I, Poirel VJ, Mendoza J, Simonneaux V. Evidence for a putative circadian Kiss-Clock in the hypothalamic AVPV in female mice. Endocrinology. 2015; 156:2999-3011.
55. Shao S, Zhao H, Lu Z, Lei X, Zhang Y. Circadian rhythms within the female HPG axis: From physiology to etiology. Endocrinology. 2021; 162.
56. Sng JC, Taniura H, Yoneda Y. Inhibition of histone deacetylation by trichostatin a intensifies the transcriptions of neuronal c-fos and c-jun genes after kainate stimulation. Neurosci Lett. 2005; 386:150-155.
57. Damaskos C, Garmpis N, Valsami S, *et al.* Histone deacetylase inhibitors: An attractive therapeutic strategy against breast cancer. Anticancer Res. 2017; 37:35-46.
58. Li X, Xu W. HDAC1/3 dual selective inhibitors - New therapeutic agents for the potential treatment of cancer. Drug Discov Ther. 2014; 8:225-228.
59. Zhou N, Xu W, Zhang Y. Histone deacetylase inhibitors merged with protein tyrosine kinase inhibitors. Drug Discov Ther. 2015; 9:147-155.
60. Hewitt SC, Korach KS. Oestrogen receptor knockout mice: Roles for oestrogen receptors alpha and beta in reproductive tissues. Reproduction. 2003; 125:143-149.
61. Wang C, Fu M, Angeletti RH, Siconolfi-Baez L, Reutens AT, Albanese C, Lisanti MP, Katzenellenbogen BS, Kato S, Hopp T, Fuqua SA, Lopez GN, Kushner PJ, Pestell RG. Direct acetylation of the estrogen receptor alpha hinge region by p300 regulates transactivation and hormone sensitivity. J Biol Chem. 2001; 276:18375-18383.

Received August 15, 2022; Revised October 14, 2022; Accepted October 20, 2022.

[§]These authors contributed equally to this work.
*Address correspondence to:
Yan Sun, Hospital & Institute of Obstetrics and Gynecology, Fudan University, 128 Shenyang Road, Yangpu, Shanghai 200081, China.
E-mail: ysunsh@126.com

Ling Wang, Laboratory for Reproductive Immunology, Obstetrics and Gynecology Hospital of Fudan University, 419 Fangxie Road, Shanghai 200011, China.
E-mail: Dr.wangling@fudan.edu.cn

Released online in J-STAGE as advance publication October 23, 2022.